

**MULTIGIGAHERTZ MONOLITHIC GAAS OPTOELECTRONIC
RECEIVERS USING 0.2 μ m GATE-LENGTH MESFETS***

R.H. Walden, W.W. Hooper, C.S. Chou, C. Ngo, R. WongQuen,
R.A. Metzger, F. Williams, L.E. Larson and R. Blumgold¹

Hughes Research Laboratories

Malibu, CA 90265

¹R. Blumgold is with Wright Laboratories, Dayton OH

Abstract: Two GaAs optical receiver front-ends are reported. Each consists of an MSM photodetector and a transresistance amplifier that drives a 50 Ω load. One amplifier has a measured analog bandwidth of 6.5 GHz and the other 4.5 GHz. The transresistance-bandwidth product for both is a very high 2.1 THz- Ω .

Optoelectronic integrated circuit (OEIC) receivers are potentially useful in high speed (5 Gb/s - 10 GB/s) optical communication systems because of their reduced parasitic capacitances and small size [1]. A popular wide-bandwidth receiver front-end architecture consists of a metal-semiconductor-metal (MSM) photodetector and a transresistance amplifier. An MSM photodetector is preferred over a PIN diode because of its low capacitance [2] and its fabrication simplicity [1], while a transresistance amplifier is used because it offers a relatively wide bandwidth and high dynamic range [3]. A high performance fabrication technology will further improve bandwidth. As an example, short-wavelength receivers, which are applicable to short-distance optical interconnect systems, can be integrated using a short gate-length GaAs MESFET process. Indeed, the widest bandwidth OEIC front-ends yet reported have utilized this approach, achieving 4.5 GHz - 5.2 GHz [2], [4]. In order to reduce the capacitance of the transresistance amplifier input node the photodetectors in these circuits had extremely small areas (10 μ m x 10 μ m [2], 15 μ m x 15 μ m [4]). Inductive peaking, commonly employed in hybrid optical receivers [5], [6] has been applied to an integrated GaAs FET transresistance amplifier [7] and a bandwidth of 7 GHz has been achieved; the equivalent unpeaked bandwidth was \approx 3.5 GHz.

In this paper, we report two different OEIC front-end designs that use an MSM

photodetector and a transresistance amplifier, represented by the feedback amplifier schematic in Fig. 1. Neither design utilizes inductive peaking. The front-ends differ in the details of the core amplifier with voltage gain, $-A$, and in the size of the MSM photodetectors.

CG027-10-14R1

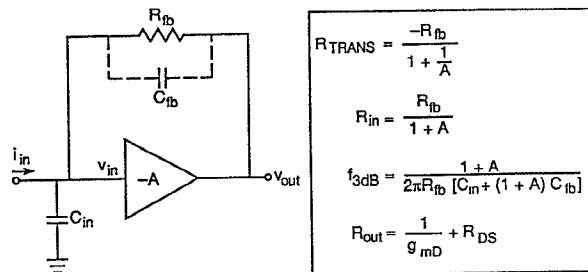


Figure 1. Schematic illustration of basic transresistance amplifier.

The MSM photodetector is represented in Fig. 1 by the photocurrent, i_{in} , flowing into the input node, and by a contribution to the input capacitance, C_{in} . The remainder of C_{in} is due primarily to the gate of the input FET (contained in the core amplifier). Relationships for the transresistance, R_{TRANS} , input resistance, R_{in} , bandwidth, f_{3dB} , and output resistance, R_{out} , are also given in Fig. 1, where R_{fb} is the feedback resistance and C_{fb} is the parasitic capacitance that shunts it. Note that if $-A \gg 1$, then $R_{TRANS} \approx -R_{fb}$.

There are two figures of merit that can be used to characterize receiver performance. One is the transresistance-bandwidth product [2], $TRBW$, which is given by

$$TRBW = |R_{TRANS}|f_{3dB} = A / (2\pi C_{tot}) \quad (1)$$

where $C_{tot} = C_{in} + (1+A)C_{fb}$. The other, which relates to receiver sensitivity, is the ratio [3],

$$SR = g_{m,in} / C_{tot}^2 \quad (2)$$

where $g_{m,in}$ is the transconductance of the input FET. The sensitivity of the receiver

*This work was supported by Wright Laboratories, Wright-Patterson Air Force Base, Dayton, OH under contract F33615-87-C-1546

is defined as the received optical power in dBm required to achieve a given bit-error rate (the ratio of incorrectly received bits to the total bits sent). TRBW and SR both benefit by making C_{tot} low. In addition, most amplifier gains will increase with increasing g_m . Hence, the use of short gate-length devices, which have high g_m and high unity-current-gain frequency, f_T , are recommended.

Our type-I receiver, shown in Fig. 2a, is based on a relatively straightforward GaAs amplifier design. The distinctive features are (1) the ratio of the gate capacitance of the input FET ($W = 100 \mu\text{m}$) to that of the photodetector is ≈ 3 , which optimizes the sensitivity [8]; and (2) the output follower is made up of 200 μm wide FETs in order to drive 50 Ω without an appreciable loss of gain.

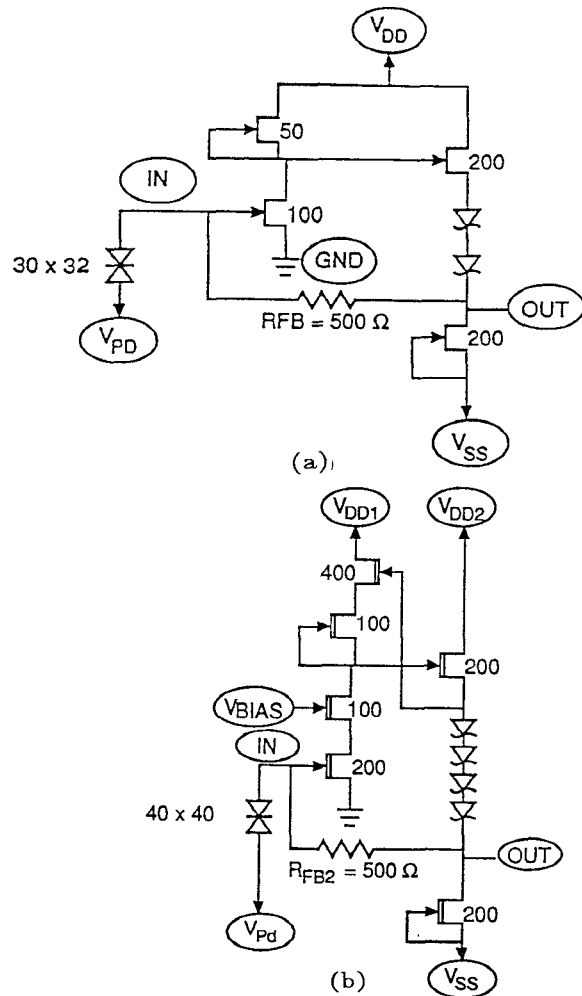


Figure 2. Circuit diagrams for (a) type-I receiver and (b) type-II receiver.

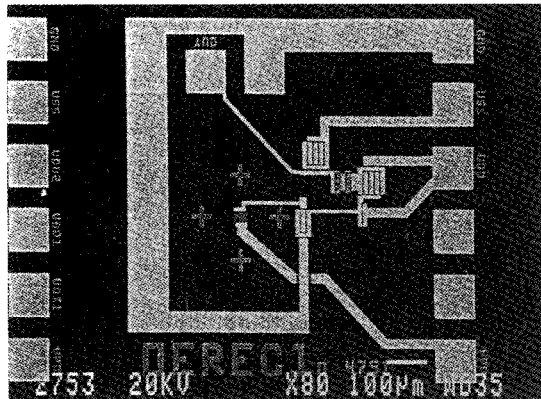
In addition to high g_m and f_T , a short channel FET will usually have a relatively high output conductance, g_{ds} , which will be

even higher at microwave frequencies than at dc. This is detrimental to achieving high A values. Our second design, shown in Fig. 2b, addresses this problem by using cross-coupled feedback to effectively double the voltage gain. In anticipation of higher A, we used a larger area detector and a wider ($W = 200 \mu\text{m}$) input FET relative to the type-I design. The design goal for R_{fb} was 500 Ω in both receivers.

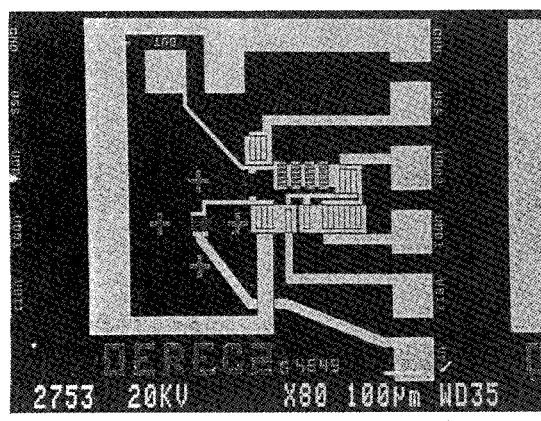
Our OEIC front-ends were fabricated with a very high performance GaAs MESFET process [9]. High performance was achieved through the use of specially designed epitaxial layers, grown by molecular beam epitaxy (MBE). The Schottky gate, formed by E-beam direct-write, was recessed into the epitaxial layers, resulting in a self-aligned MESFET structure having very low parasitic resistance (0.05 Ωmm) and a high g_m . Ohmic contacts were formed by evaporated AuGe/Ni/Au, and the gate metalization was Ti/Pt/Au. Interelectrode device and circuit capacitances were minimized by the use of plated Au air bridges. A typical MESFET was characterized by a gate-length of 0.2 μm , $g_m = 480 \text{ mS/mm}$, $f_T = 60 \text{ GHz}$, and a threshold voltage of -0.75 V. Fabrication of the MSM photodetectors was accomplished simply by recessing the active detector area into the semi-insulating (SI) GaAs substrate and depositing the Schottky electrodes. Figure 3 shows SEM micrographs of the fabricated type-I and type-II receiver circuits.

The MSM photodetectors consisted of interdigitated metal electrodes on SI GaAs. The electrode width was 1 μm and the interelectrode gap was 3 μm . The type-I receiver (Fig. 3a) contains a 30 $\mu\text{m} \times 32 \mu\text{m}$ photodetector and the type-II circuit (Fig. 3b) a 40 $\mu\text{m} \times 40 \mu\text{m}$ photodetector. Standalone MSM test patterns were included in the mask set, and S-parameter measurements were made on these patterns in a two-port configuration. The -3 dB frequencies of the input return loss, S_{11} , were 45 GHz and 35 GHz, corresponding to low photodetector capacitances of 35 fF and 45 fF, for the 30 $\mu\text{m} \times 32 \mu\text{m}$ and the 40 $\mu\text{m} \times 40 \mu\text{m}$ patterns respectively. The photoresponse of the photodetectors was measured using an Ortel SL620 laser with a 840 nm wavelength coupled to an optical fiber. Responsivities of $\approx 0.36 \text{ mA/mW}$ and $\approx 0.45 \text{ mA/mW}$ were obtained for the 30 $\mu\text{m} \times 32 \mu\text{m}$ and 40 $\mu\text{m} \times 40 \mu\text{m}$ patterns respectively. The frequency response was obtained by modulating the laser with a -5 dBm signal from a Wilmtron model 360 network analyzer. The forward transmission, S_{21} , for the smaller MSM photodetector illuminated at full laser power ($\approx 4 \text{ mW}$) is shown as the lower curve in Fig. 4a. S_{21} for the larger photodetector illuminated at half power is shown as the lower curve in Fig. 4b. The lower curves in Fig. 4 represent the combined response of the laser and the photodetectors. Part of the gradual low-

frequency rolloff and almost all of the high frequency rolloff beyond 7 GHz, is due to the laser, indicating that S_{21} for a photodetector alone has a relatively gentle decline with increasing frequency which is typical of MSM detectors on SI GaAs. Apart from this effect, the MSM bandwidth is estimated to be ≈ 10 GHz, and does not limit receiver performance.



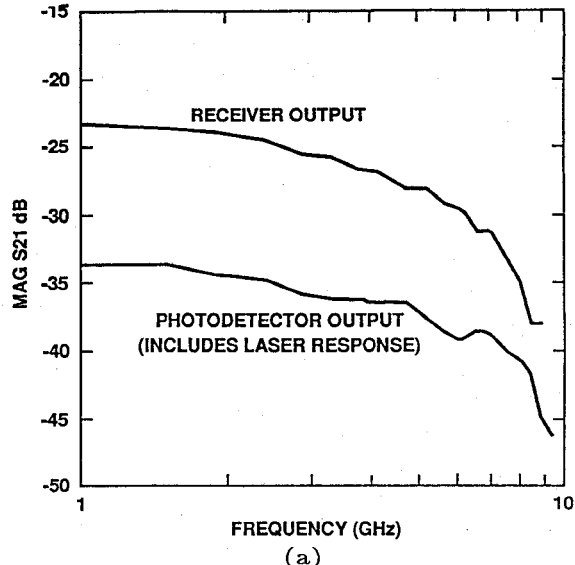
(a)



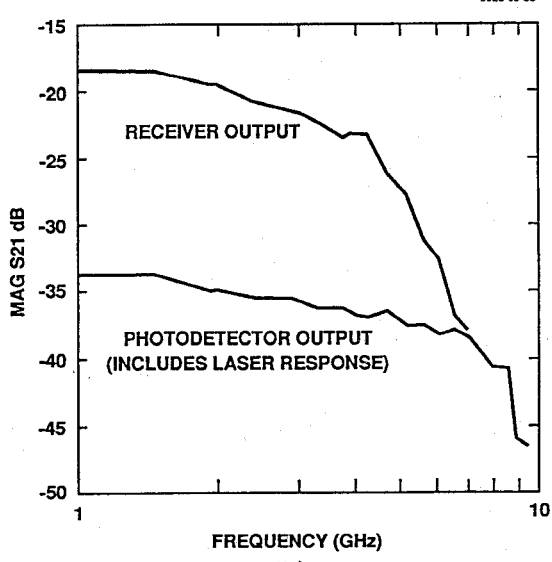
(b)

Figure 3. SEM micrographs for (a) type-I receiver and (b) type-II receiver.

We evaluated the receivers under illumination using the same conditions as for the photodetectors. Representative $|S_{21}|$ data are shown as the upper curves in Figs. 4a and 4b for the type-I and type-II circuits respectively. The responses of the transresistance amplifiers are obtained by subtracting the detector plus laser curves from the receiver curves and are shown in Fig. 5. It is determined that the 3 dB bandwidths are ≈ 6.5 GHz and ≈ 4.5 GHz for type-I and type-II respectively. It is also seen that the type-II receiver has 5 dB higher gain. S-parameter measurements on standalone transresistance amplifier test



(a)



(b)

Figure 4. Frequency responses of illuminated receivers, (a) type-I, (b) type-II. Each graph also contains the appropriate MSM plus laser response.

circuits on the same wafer confirm these results.

The important circuit parameters, deduced from the S-parameter data, are summarized in Table I.

Table I. Receiver Parameters

Type	R_{FB}	R_{TRANS}	C_{tot}	$-A$	f_{3dB}
I	520 Ω	330 Ω	130fF	1.8	6.5GHz
II	600 Ω	460 Ω	270fF	3.5	4.5GHz

The values for R_{TRANS} , R_{fb} , and A were determined at 1 GHz instead of at DC in

order to fully account for the effects of the frequency dependent degradation in output conductance. A very high value of $TRBW \approx 2.1 \text{ THz-}\Omega$ is found for both receivers. The SR values are 2.8 S/pF^2 and 1.3 S/pF^2 for the type-I and type-II receivers respectively. The performance of the type-I receiver as characterized by f_{3dB} , $TRBW$, and SR is perhaps the highest yet reported for an OEIC. The type-II receiver also has high performance figures, and, due to its larger detector area and higher $|S_{21}|$, will produce an output voltage that is about three times larger than that of the type-I receiver for a given input power level.

In summary, two OEIC receivers with MSM photodetectors and MESFET transresistance amplifiers were fabricated in a 60 GHz GaAs process. The transresistance-bandwidth product for both circuits and the bandwidth of one of them are the highest yet reported for OEICs.

References

- [1] M. Dagenais, R.F. Leheny, H. Temkin, and P. Bhattacharya, "Applications and challenges of OEIC technology: a report on the 1989 Hilton Head Workshop," *J. Lightwave Technol.*, LT-8, p. 846, June 1990.
- [2] C.S. Harder, B. Van Zeghbroeck, H. Meier, W. Patrick, and P. Vettiger, "5.2 GHz bandwidth monolithic GaAs optoelectronic receiver," *IEEE Electron Dev. Lett.*, EDL-9, p.171, April 1988.
- [3] R.G. Smith and S.D. Personick, "Receiver design for optical fiber communication systems," in *Semiconductor Devices for Optical Communication*, H. Kressel, Ed., Springer-Verlag, p. 89, 1982.
- [4] E. Sano, "A device model for metal-semiconductor-metal photodetectors and its applications to optoelectronic integrated circuit simulation," *IEEE Trans. Electron Dev.*, ED-37, P.1964, Sept. 1990.
- [5] J.L. Gimlett, "Ultrawide bandwidth optical receivers," *J. Lightwave Technol.*, LT-7, p. 1432, Oct. 1989.
- [6] N. Ohkawa, "Fiber-optic multigigabit GaAs MIC front-end circuit with inductive peaking," *J. Lightwave Technol.*, LT-6, p.1665, 1988.
- [7] Y. Miyagawa, Y. Miyamoto, and K. Hagimoto, "7 GHz bandwidth optical front-end circuit using GaAs FET monolithic IC technology," *Electron. Lett.*, vol. 25, p. 1305, Sept. 1989.
- [8] R.A. Minasian, "Optimum Design of a 4-Gbit/s GaAs MESFET optical preamplifier," *J. Lightwave Technol.*, LT-5, p. 373, March 1987.
- [9] L.E. Larson, C.S. Chou and M.J. Delaney, "An ultrahigh-speed GaAs MESFET operational amplifier," *IEEE J. Solid-State Circuits*, SC-24, p.1523, Dec. 1989.

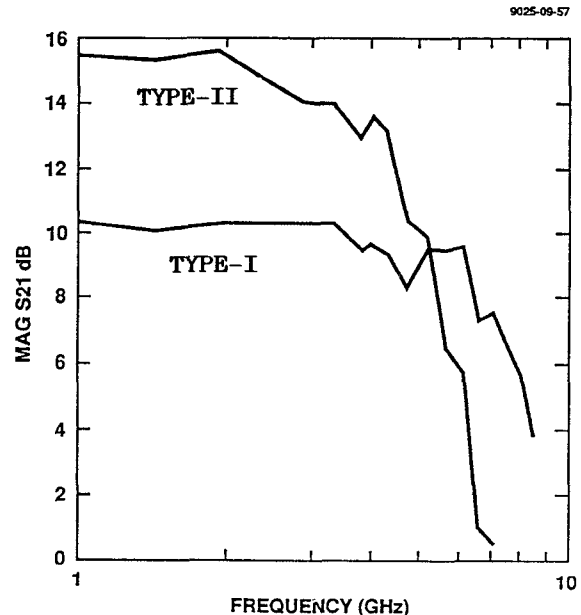


Figure 5. Net response of transresistance amplifiers under illumination.